

A NEARBY OLD HALO WHITE DWARF CANDIDATE FROM THE SLOAN DIGITAL SKY SURVEY

PATRICK B. HALL,¹ PIOTR M. KOWALSKI,² HUGH C. HARRIS,³ AKSHAY AWAL,^{1,4} S. K. LEGGETT,⁵ MUKREMIN KILIC,⁶
SCOTT F. ANDERSON,⁷ EVALYN GATES⁸

ABSTRACT

We report the discovery of a nearby, old, halo white dwarf candidate from the Sloan Digital Sky Survey. SDSS J110217.48+411315.4 has a proper motion of 1.75"/year and redder optical colors than all other known featureless (type DC) white dwarfs. We present SDSS imaging and spectroscopy of this object, along with near-infrared photometry obtained at the United Kingdom Infra-Red Telescope. Fitting its photometry with up-to-date model atmospheres, we find that its overall spectral energy distribution is fit reasonably well with a pure hydrogen composition and $T_{\text{eff}} \approx 3800$ K (assuming $\log g = 8$). That temperature and gravity would place this white dwarf at 35 pc from the Sun with a tangential velocity of 290 km s⁻¹ and space velocities consistent with halo membership; furthermore, its combined main sequence and white dwarf cooling age would be ≈ 11 Gyr. However, if this object is a massive white dwarf, it could be a younger object with a thick disk origin. Whatever its origin, the optical colors of this object are redder than predicted by any current pure hydrogen, pure helium or mixed hydrogen-helium atmospheric model, indicating that there remain problems in our understanding of the complicated physics of the dense atmospheres of cool white dwarfs.

Subject headings: stars: individual (SDSS J110217.48+411315.4) — white dwarfs

1. INTRODUCTION

There is considerable interest in white dwarf (WD) stellar remnants in the halo of our Galaxy. Since halo stars are generally older than disk stars, the oldest halo WDs should be older and cooler than the oldest disk WDs. Such objects are of interest for studying the age distribution of halo stars and for testing our understanding of stellar atmospheres, since their spectra can depart significantly from simple blackbodies (see, e.g., Hansen 1998; Saumon & Jacobson 1999; Kowalski 2006a). Halo WD candidates may be identifiable as faint objects with high proper motions and unusual colors (e.g., Ducourant et al. 2007). Some halo WD candidates have indeed been found, but most of them have relatively warm temperatures, indicating they are relatively young white dwarfs (e.g., Bergeron et al. 2005; Lépine, Rich, & Shara 2005). To date, the coolest known *probable* halo WD is WD 0346+246, with $T \simeq 3800$ K (Bergeron 2001). The coolest halo WD *candidate*, whose velocities are consistent either with a halo or a thick disk origin, is SDSS J122048.65+091412.1 (Gates et al. 2004). The latter object is one of a handful of *ultracool* WDs ($T_{\text{eff}} \lesssim 3800$ K) whose optical spectra show collision-induced absorption (CIA) from H₂. CIA causes WDs to exhibit increasingly bluer colors at increasingly shorter wavelengths at

$T_{\text{eff}} \lesssim 5000$ K (see, e.g., Bergeron et al. 2005).

Here we report the identification of a candidate old, halo WD with red optical colors whose spectrum was obtained by the Sloan Digital Sky Survey (SDSS; York et al. 2000). The SDSS used a drift-scanning imaging camera (Gunn et al. 1998) on a 2.5-m telescope (Gunn et al. 2006) to image $\sim 10^4$ deg² of sky on the SDSS *ugriz* magnitude system (Fukugita et al. 1996; Hogg et al. 2001; Smith et al. 2002; Pier et al. 2003; Ivezić et al. 2004; Tucker et al. 2006). Two multi-fiber, double spectrographs are being used to obtain $R \sim 2100$ spectra for $\sim 10^6$ galaxies and $\sim 10^5$ quasar candidates (Stoughton et al. 2002). As discussed in Richards et al. (2002), most quasar candidates are targeted for spectroscopy because they are outliers from the stellar locus. Spectroscopy of such targets provides data not just on quasars, but also on objects with colors different from those of the stellar locus, such as the unusual white dwarf presented herein.

2. IMAGES AND PHOTOMETRY

SDSS J110217.48+411315.4 (hereafter J1102+4113)⁹ was noticed during visual inspection of all SDSS spectra from Data Release Six (Adelman-McCarthy et al. 2008) classified as UNKNOWN by the SDSS pipeline. It stood out in the SDSS Catalog Archive Server as having a high proper motion of $\mu_{\alpha} = -105.0 \pm 3.5$ milliarcsec year⁻¹ and $\mu_{\delta} = -1750 \pm 3.5$ milliarcsec year⁻¹, computed as described in Munn et al. (2004) by combining astrometry from the SDSS and from the USNO-B1.0 catalog (Monet et al. 2003). J1102+4113 is present in seven Palomar Observatory Sky Survey (POSS) plates and is present in one published SDSS observation. A selection of these images is shown in Figure 1. J1102+4113 is catalogued

⁹ Due to its high proper motion, the SDSS coordinates for this object are in Equinox J2000 and Epoch 2003.3. The United States Naval Observatory USNO-B1.0 coordinates for this object in Equinox J2000 and Epoch 2000 are RA=11:02:17.50 and DEC=+41:13:21.52.

¹ Department of Physics and Astronomy, York University, Toronto, Ontario M3J 1P3, Canada

² Lehrstuhl für Theoretische Chemie, Ruhr-Universität, 44780 Bochum, Germany

³ United States Naval Observatory, Flagstaff, AZ 86001, USA

⁴ Emery Collegiate Institute, Toronto, Ontario M9M 2V9, Canada

⁵ Gemini Observatory, 670 North A'ohoku Place Hilo, HI 96720, USA

⁶ Department of Astronomy, The Ohio State University, Columbus, OH 43210, USA

⁷ Department of Astronomy, University of Washington, Seattle, WA 98195, USA

⁸ Kavli Institute for Cosmological Physics, The University of Chicago, Chicago, IL 60637, USA

in USNO-B1.0 as 1312-0217226, with proper motions of $\mu_\alpha = -106 \pm 2$ milliarcsec year⁻¹ and $\mu_\delta = -1744 \pm 1$ milliarcsec year⁻¹ based on 5 photographic epochs only. We adopt a total proper motion of $\mu = 1.75$ arcsec year⁻¹. In Galactic coordinates, J1102+4113 is located above the Galactic plane near anticenter ($l, b = 174^\circ, 63.5^\circ$). Its proper motion is predominantly in the $+l$ direction. Taken together, those findings mean that its velocity parallel to the Galactic plane is less than the Sun's (see §4.1).

Despite its presence in the USNO-B1.0 catalog, this object has not been reported in the literature as a high-proper-motion star. No sources are listed in the SIMBAD or NED databases within $1'$ of its position. J1102+4113 is bright enough that it could have been found by Luyten (1974). It was missed during examination of USNO-B high-proper-motion stars by Levine (2005) because it is 0.3 mag fainter than the limit of $R < 18.0$ used in that study. It should also have been found in the LSPM-N catalog (Lépine, Shara, & Rich 2003; Lépine & Shara 2005), although it is near the lower magnitude limit and upper proper motion limit of that catalog. It may have been missed by previous searches because the image on the POSS-I E plate appears double (Figure 1, top left panel). This is likely due to a plate flaw, since the second component of the putative double is narrower than the point spread function.

Available photometry from published observations of J1102+4113 is given in Table 1. The object is consistently faint in blue passbands. There is a faint J -band feature in the Two Micron All Sky Survey (2MASS; Skrutskie et al. 2006) within $2''$ of the expected position of J1102+4113 at that epoch. To measure the flux in this feature, we retrieved the 2MASS Atlas images covering this object, measured $3''$ radius aperture magnitudes in J , H and K_s at the position of the potential J -band detection, and calculated appropriate magnitude uncertainties.¹⁰ These measurements are included in Table 1, but their large uncertainties make them of limited use. To obtain better near-infrared constraints, we obtained JHK photometry of J1102+4113 on 2007 December 21 using the United Kingdom Infrared Telescope (UKIRT) Fast-Track Imager (UFTI; Roche et al. 2003) in service mode. The data were reduced in the standard fashion and the photometry was calibrated using observations of UKIRT faint standard #130 (Leggett et al. 2006). These measurements are also included in Table 1.

3. SPECTRA

Based on initial ('TARGET') photometric reductions of SDSS imaging, J1102+4113 was targeted as a high-redshift quasar candidate (target flag QSO_HIZ). A single SDSS spectrum was obtained on Modified Julian Date (MJD) 53046 on SDSS spectroscopic plate No. 1437 and fiber No. 428. In Figure 2 we present the full SDSS spectrum of J1102+4113. Its spectrum is red and featureless (in particular, there is no sign of Balmer absorption) except for a possible broad emission feature at 5750–5900 Å. This feature is near one end of the wavelength region 5800–6150 Å where both the blue and red SDSS spec-

trographs record flux from an object. To investigate the reality of this feature, we examined the four individual blue and red exposures which were all combined to produce the final weighted average SDSS spectrum shown in Figure 2. The broad feature is present in each of the four individual blue exposures, but not in any of the four individual red exposures. In fact, the red exposures all show a dip in flux below 6050 Å. In Figure 3 we present the average spectra of this object obtained with the blue and red SDSS spectrographs, shown in blue and red respectively, along with the $\pm 1\sigma$ uncertainties for both spectra, shown in gray. The flux levels at 5800–6000 Å in the two spectra do not agree within the uncertainties. This disagreement is indicative of some problem with the SDSS spectrum in this wavelength range. We conclude that the broad feature at 5750–5900 Å is an artifact,¹¹ although an independent spectrum would still be worth obtaining to verify that conclusion.

There is no other statistically significant absorption or emission feature in the spectrum. In particular, there is no sign of H α absorption to a 3σ limit of ~ 0.8 Å. (The smoothed spectrum shows a dip in flux at 6522 Å, but it is due to two noise spikes which are narrower than the instrumental resolution.)

4. ANALYSIS AND COMPARISON WITH MODELS

We classify J1102+4113 as a DC WD, since its optical spectrum has no robust features. The featureless spectrum of J1102+4113 is similar to other cool DC WDs. At optical wavelengths, the reddest of these are WD 0346+246 (Oppenheimer et al. 2001b), GD 392B (Farihi 2004), WD 1247+550 (Liebert, Dahn, & Monet 1988) and WD 1310-472 (Bergeron, Leggett, & Ruiz 2001). These four stars all have $B - V \simeq 1.4$ and $1.39 < V - I < 1.46$.¹² Only one of these four WDs has a measured $g - i$ color, but the small dispersion in their $V - I$ colors means there will be a small dispersion in their $g - i$ colors. Thus, comparing the $g - i = 1.67$ measured for WD 1247+550 with the $g - i = 1.99$ measured for J1102+4113, we conclude that J1102+4113 is $\simeq 0.3$ mag redder in $g - i$ than the reddest previously known DC white dwarfs. The only other non-magnetic WDs¹³ known to have optical colors approaching those of J1102+4113 are DZ WDs with extremely strong calcium and sodium absorption: WD 2251-070 (Liebert et al. 1988), WD J2356-209 (Oppenheimer et al. 2001a) and SDSS J133001.13+643523.8 (Harris et al. 2003). In contrast, J1102+4113 shows no evidence of absorption from Na I $\lambda\lambda 5891, 5897$, Ca I $\lambda 4227$ Å or Ca II $\lambda\lambda 8500, 8544, 8664$ Å. A cool atmosphere with an

¹¹ Some pixels at nearby wavelengths are flagged as potentially being untrustworthy, with some or all of the flags NEARBADPIXEL, LOWFLAT, SCATTEREDLIGHT, BADFLUXFACTOR, and BADSKYCHI (Stoughton et al. 2002). Empirically, we have found that the grow radius around such untrustworthy pixels is, on rare occasions, not large enough to flag all apparently problematic pixels in SDSS spectra. This spectrum may be one such case.

¹² Two WDs reported to have $V - I > 1.5$ by Oswalt et al. (1996) in fact have $V - I < 1.0$ (Bergeron et al. 2001; Harris, unpublished).

¹³ No known magnetic WD has a red, featureless spectrum like that of J1102+4113. Nonetheless, polarimetric observations would be useful to ensure that J1102+4113 is not some sort of unusual magnetic WD.

¹⁰ The calculation of the magnitude uncertainties followed the procedure in section VI.8.a.ii of the 2MASS Explanatory Supplement at <http://www.ipac.caltech.edu/2mass/releases/allsky/doc/explsup.html>.

extremely low metal abundance seems the best explanation for its red color.

For a surface temperature as low as that indicated by the red color of J1102+4113, both pure hydrogen and pure helium model atmospheres are expected to be essentially featureless in the optical. In cool, pure H atmospheres, most H is in the form of H_2 and most atomic H is in the ground state, leading to negligible Balmer absorption (which would be extremely pressure broadened in any case). In cool, pure He atmospheres, most He is neutral and the lower levels of optical transitions of He I are not populated for $T_{\text{eff}} \lesssim 12,000$ K, leading to highly optically transparent atmospheres. Nonetheless, there can be detectable differences between the spectra of hydrogen- and helium-dominated cool WDs, particularly in the near-infrared where collision-induced absorption is affected by the composition.

To constrain the atmospheric composition of J1102+4113, we fit model WD atmospheres to the UKIRT photometry and to the SDSS photometry converted to an AB system. The SDSS magnitudes are already on an AB system to within $\simeq 1\%$ in g and r , while in other bands we applied the corrections $u_{AB} = u_{SDSS} - 0.04$, $i_{AB} = i_{SDSS} + 0.02$ and $z_{AB} = z_{SDSS} + 0.03$ (Abazajian et al. 2004; Eisenstein et al. 2006; cf. Holberg 2007; Holtzman et al. 2008, in preparation). To account for the $\simeq 1\%$ uncertainties in these corrections, we increased the uncertainties from 2% to 3% for each SDSS magnitude besides u in the fitting.

In Figure 4 we plot the SDSS spectrum of J1102+4113, the SDSS and UKIRT photometry and synthetic photometry from fits discussed below, all in units of flux density per unit frequency versus wavelength. For illustrative purposes, the spectrum has been scaled upwards by 0^m6 to match the optical photometry. Such scaling is needed because not all the light from the object is captured by the spectroscopic fiber. The scaling is greater than the typical SDSS value of 0^m35 (Adelman-McCarthy et al. 2008), probably because the fiber placement did not account for the $1''.4$ proper motion of J1102+4113 between the imaging and spectroscopic epochs.

4.1. Comparison with Pure Hydrogen Models

We first fit pure-hydrogen atmosphere models (Kowalski 2006b; Kowalski & Saumon 2006; Kowalski 2007) to the photometry of J1102+4113 (excluding the u band, whose uncertainties are too large to be useful), assuming a typical WD gravity of $\log g = 8$ (e.g., Fontaine, Brassard, & Bergeron 2001). The resulting fit yields $T_{\text{eff}} = 3830$ K. Synthetic photometry from this model is shown as the blue triangles in Figure 4. The fit is reasonable given the model uncertainties, although the formal χ^2 is quite poor: $\chi^2 = 111$ for 4 degrees of freedom ($\nu = n - 1 = 6$ minus T_{eff} minus a normalization factor), with about $\sim 75\%$ of the χ^2 signal coming from the discrepancy at g . The red optical colors are produced in the far red wing of $\text{Ly}\alpha$ (perturbed at high density), while the dips in the near-IR spectrum are due to H_2 - H_2 collision-induced absorption (CIA).

While J1102+4113 is 0^m22 redder in $g - z$ than any pure-H model, it is an open question how well such models reproduce the relevant physics at $T_{\text{eff}} \simeq 3800$ K. Hy-

drogen in the atmosphere of a $T_{\text{eff}} \simeq 3800$ K WD is approaching a density where nearby molecules are strongly correlated and where the refractive index is significantly greater than unity. Furthermore, there are still uncertainties about the reliability of H_2 CIA opacities in WDs. Observationally, there are few WDs known near that temperature with which comparisons with models can be made. At $T_{\text{eff}} \lesssim 3800$ K, CIA will affect the optical colors of WDs and their $g - z$ colors will become bluer. However, given all the physical effects discussed above that may not be handled correctly in the models, it is not certain how optically red pure-H atmospheres become before they turn bluer. In short, the models could be sufficiently in error to explain the formally poor fit of the pure H model predictions to the J1102+4113 data.

The distance to the WD in our pure-H model fit is 35 pc, making the tangential velocity $v_{\text{tan}} = 290$ km s^{-1} . The cooling time to reach $T_{\text{eff}}=3830$ K is ≈ 9.6 Gyr, assuming a typical WD mass of $0.6 M_{\odot}$ with a core of equal parts C and O (Fontaine et al. 2001). Including ≈ 1 Gyr for its progenitor's lifetime (Fontaine et al. 2001), for a pure-H model J1102+4113 is the remnant of a star that formed ≈ 11 Gyr ago. Alternatively, at the same temperature, if $\log g = 9$ (9.5), then J1102+4113 would have the following approximate properties: $M = 1.11$ (1.36) M_{\odot} , $d = 17$ (10) pc, $v_{\text{tan}} = 140$ (83) km s^{-1} , cooling time 7 (3) Gyr and progenitor lifetime $\ll 1$ Gyr. If J1102+4113 has $\log g = 7.5$, then it would be at $d = 42$ pc with $M = 0.35 M_{\odot}$ and its total age would be greater than the age of the universe unless it is an unresolved double degenerate or a product of common-envelope binary star evolution (Fontaine et al. 2001).

We can calculate the components of the object's space velocity relative to the Sun, U , V and W , which are positive in the directions of Galactic Center, Galactic rotation, and the North Galactic Pole, respectively. If we assume zero radial velocity we find $(U, V, W) = (63, -280, 46)$ km s^{-1} for $d = 35$ pc, $(30, -140, 22)$ km s^{-1} for $d = 17$ pc, and $(18, -80, 13)$ km s^{-1} for $d = 10$ pc. Chiba & Beers (2000) give $(\langle U \rangle, \langle V \rangle, \langle W \rangle) = (17 \pm 141, -187 \pm 106, -5 \pm 94)$ km s^{-1} for the halo and $(4 \pm 46, -20 \pm 50, -3 \pm 35)$ km s^{-1} for the thick disk. Thus, the space velocities of J1102+4113 are most consistent with those of the halo. However, if J1102+4113 is at $d \lesssim 13.5$ pc, it could be a young, thick disk WD with an unusually (but not unprecedentedly) high mass. A parallax measurement is needed to discriminate between these possibilities and to pin down the mass of J1102+4113.

4.2. Comparison with Pure Helium Models

We next fit pure He models (Kowalski & Saumon 2004, 2006) to the data (again assuming $\log g = 8$), but were not able to find a realistic fit. If the near-infrared photometry is omitted, a good fit is found with $T_{\text{eff}}=3360$ K. Synthetic photometry from this model is shown as the red squares in Figure 4; the model near-infrared fluxes greatly overpredict the observed fluxes. Thus, a good fit cannot be found to the combined optical and near-IR photometry of J1102+4113 with a pure He model: if the temperature is increased to move the peak of the fit to shorter wavelengths, the slope of the optical fit will deviate unacceptably from the observations (see the blue

lines in Figure 5).

4.3. Comparison with Mixed Hydrogen-Helium Models

We also consider mixed H/He models, as even a tiny amount of hydrogen in a helium-dominated atmosphere ($H/He \gtrsim 10^{-10}$) can induce sufficient H_2 -He CIA to cause a significant near-infrared flux deficit (see, e.g., Figure 5 of Bergeron & Leggett 2002). The results of normalizing mixed H/He models with $T_{\text{eff}} = 3500$ K to the photometry are shown in Figure 5; for slightly higher or lower T_{eff} (± 500 K) the overall results are similar. None of the mixed H/He models yield a better match to the data than the pure hydrogen model, although a model with $H/He = 10^{-5}$ fits at wavelengths $\lambda < 1.5$ microns.

In summary, the poor fit of pure-He models to the photometry means that there is certainly hydrogen in the atmosphere of this WD. However, the H/He ratio cannot be pinned down with current models, due to uncertainties in how accurately the models treat the complicated physics involved (refraction, non-ideal equation of state, non-ideal chemistry, perturbed Lyman series absorption, etc.; see Kowalski 2006a). Both $H/He \gg 1$ and $H/He \ll 1$ are possible.

4.4. Modeled and Observed Fluxes and Colors

If only observational uncertainties are considered, no current WD model atmosphere provides a formally acceptable fit to the photometry of J1102+4113. To guide future models, it is worth examining at what wavelengths the discrepancies arise.

In both Figures 4 and 5, it can be seen that J1102+4113 is redder at optical wavelengths than most model fits. To even approximately match both the red optical colors and the depression of the near-infrared flux (relative to a blackbody of the same temperature) requires some hydrogen in its atmosphere.

In terms of $u - g$ vs. $g - z$, J1102+4113 matches neither pure-H models nor pure-He models (see Table 1 and Figure 4b of Kowalski & Saumon 2006). It is redder in $g - z$ than pure-H models at any $u - g$ but is bluer in $u - g$ than the pure-He models at its $g - z$ color. Because of the large uncertainty in its $u - g$ color, J1102+4113 is only 1.7σ redder in $u - g$ than the pure-He sequence of Kowalski & Saumon (2006).

5. SUMMARY

SDSS J110217.48+411315.4 is a cool WD with either a pure hydrogen atmosphere at $T_{\text{eff}} \simeq 3830$ K or a mixed hydrogen-helium atmosphere with $H/He \simeq 10^{-5}$ and $T_{\text{eff}} \simeq 3500$ K. In either case, its distance is expected to be $d \lesssim 40$ pc. At its best-fit distance of $d \simeq 35$ pc, its high proper motion of $1.75''/\text{year}$ makes it a member of the halo, with an estimated total age of ≈ 11 Gyr. If its distance is $d \lesssim 13.5$ pc, it could be a halo or a thick disk object. A parallax measurement for J1102+4113 is needed to settle the question of its origin and to determine its mass. To improve the data available for fitting models to J1102+4113, deeper u photometry and photometry at $\lambda > 2.5$ microns might be useful, as might optical spectroscopy with a higher signal-to-noise ratio. As for the models themselves, improvements to mixed H-He models are known to be needed. In addition, better H_2 CIA opacities (especially at optical wavelengths) and more examples of WDs at $T_{\text{eff}} \approx 4000$ K are needed to determine how well, on average, pure-H models at such temperatures match real WD atmospheres.

In principle, the SDSS can be used to place an upper limit on the surface density of red, high-proper-motion WDs like J1102+4113. In practice, additional spectroscopy beyond that obtained by the SDSS will be needed to place such a limit, because objects like J1102+4113 have colors too similar to those of the stellar locus to be routinely selected for SDSS spectroscopy. (J1102+4113 itself barely qualified as a quasar candidate based on preliminary ('TARGET') SDSS imaging reductions, and no longer qualified for spectroscopy based on final ('BEST') reductions.) J1102+4113 is the only $g < 19.7$, $g - r > 1.4$ object in the 8417 deg² SDSS DR6 Legacy imaging database with SDSS+USNO-B1.0 proper motion $\mu \geq 1.5''/\text{year}$ (Munn et al. 2004), but similarly red objects with $\mu \lesssim 1''/\text{year}$ that lack SDSS spectroscopy exist in the database. Whether or not any of those objects turn out to be WDs, J1102+4113 will remain one of the highest proper motion cool WDs in the sky as seen from Earth.

We thank D. Saumon and the anonymous referee for helpful comments. PBH was supported by NSERC and AA by the York-Seneca Summer Science and Technology Program. PMK acknowledges partial support from Ruhr Universität. SKL's research is supported by the Gemini Observatory, which is operated by the Association of Universities for Research in Astronomy, Inc., on behalf of the international Gemini partnership of Argentina, Australia, Brazil, Canada, Chile, the United Kingdom, and the United States of America.

Some of the data reported here were obtained as part of Service Programme 1771 at the United Kingdom Infrared Telescope, which is operated by the Joint Astronomy Centre on behalf of the Science and Technology Facilities Council of the U.K. This research has also made use of: the NASA/IPAC Infrared Science Archive and the NASA/IPAC Extragalactic Database (NED), which are operated by the Jet Propulsion Laboratory, California Institute of Technology, under contract with the National Aeronautics and Space Administration; the SIMBAD database, operated at CDS, Strasbourg, France; data products from the Two Micron All Sky Survey, which is a joint project of the University of Massachusetts and the Infrared Processing and Analysis Center/California Institute of Technology, funded by the National Aeronautics and Space Administration and the National Science Foundation; and the USNOFS Image and Catalogue Archive operated by the United States Naval Observatory, Flagstaff Station (<http://www.nofs.navy.mil/data/fchpix/>).

Funding for the SDSS and SDSS-II has been provided by the Alfred P. Sloan Foundation, the Participating Institutions, the National Science Foundation, the U.S. Department of Energy, the National Aeronautics and Space Administration, the Japanese Monbukagakusho, and the Max Planck Society, and the Higher Education Funding Council for England. The SDSS Web site is <http://www.sdss.org/>. The SDSS is managed by the Astrophysical Research Consortium for the Participating Institutions. The Participating Institutions are the American Museum of Natural History, Astrophysical Institute Potsdam, University of Basel, University of Cambridge, Case Western Reserve University, The University

of Chicago, Drexel University, Fermilab, the Institute for Advanced Study, the Japan Participation Group, The Johns Hopkins University, the Joint Institute for Nuclear Astrophysics, the Kavli Institute for Particle Astrophysics and Cosmology, the Korean Scientist Group, the Chinese Academy of Sciences, Los Alamos National

Laboratory, the Max-Planck-Institute for Astronomy, the Max-Planck-Institute for Astrophysics, New Mexico State University, Ohio State University, University of Pittsburgh, University of Portsmouth, Princeton University, the United States Naval Observatory, and the University of Washington.

REFERENCES

- Abazajian, K., Adelman-McCarthy, J. K., Agüeros, M. A., Allam, S. S., Anderson, K. S. J., Anderson, S. F., Annis, J., Bahcall, N. A., et al. 2004, *AJ*, 128, 502
- Adelman-McCarthy, J., Agüeros, M., Allam, S., Allende Prieto, C., Anderson, K., Anderson, S., Annis, J., Bahcall, N., et al. 2008, *ApJS*, 175, 297
- Bergeron, P. 2001, *ApJ*, 558, 369
- Bergeron, P. & Leggett, S. K. 2002, *ApJ*, 580, 1070
- Bergeron, P., Leggett, S. K., & Ruiz, M. T. 2001, *ApJS*, 133, 413
- Bergeron, P., Ruiz, M. T., Hamuy, M., Leggett, S. K., Currie, M. J., Lajoie, C.-P., & Dufour, P. 2005, *ApJ*, 625, 838
- Chiba, M. & Beers, T. C. 2000, *AJ*, 119, 2843
- Ducourant, C., Teixeira, R., Hambly, N. C., Oppenheimer, B. R., Hawkins, M. R. S., Rapaport, M., Modolo, J., & Lecampion, J. F. 2007, *A&A*, 470, 387
- Eisenstein, D. J., Liebert, J., Harris, H. C., Kleinman, S. J., Nitta, A., Silvestri, N., Anderson, S. A., Barentine, J. C., et al. 2006, *ApJS*, 167, 40
- Farihi, J. 2004, *ApJ*, 610, 1013
- Fontaine, G., Brassard, P., & Bergeron, P. 2001, *PASP*, 113, 409
- Fukugita, M., Ichikawa, T., Gunn, J. E., Doi, M., Shimasaku, K., & Schneider, D. P. 1996, *AJ*, 111, 1748
- Gates, E., Gyuk, G., Harris, H. C., Subbarao, M., Anderson, S., Kleinman, S. J., Liebert, J., Brewington, H., et al. 2004, *ApJ*, 612, L129
- Ghinassi, F., Licandro, J., Oliva, E., Baffa, C., Checcucci, A., Comoretto, G., Gennari, I. S., & Marucci, G. 2002, *A&A*, 386, 1157
- Gunn, J. E., Carr, M., Rockosi, C., Sekiguchi, M., Berry, K., Elms, B., de Haas, E., Ivezić, Ž., et al. 1998, *AJ*, 116, 3040
- Gunn, J. E., Siegmund, W. A., Mannery, E. J., Owen, R. E., Hull, C. L., Leger, R. F., Carey, L. N., Knapp, G. R., et al. 2006, *AJ*, 131, 2332
- Hansen, B. M. S. 1998, *Nature*, 394, 860
- Harris, H. C., Liebert, J., Kleinman, S. J., Nitta, A., Anderson, S. F., Knapp, G. R., Krzesiński, J., Schmidt, G., et al. 2003, *AJ*, 126, 1023
- Hogg, D., Finkbeiner, D., Schlegel, D., & Gunn, J. 2001, *AJ*, 122, 2129
- Holberg, J. B. 2007, in *Astronomical Society of the Pacific Conference Series*, Vol. 364, *The Future of Photometric, Spectrophotometric and Polarimetric Standardization*, ed. C. Sterken, 553
- Ivezić, Ž., Lupton, R. H., Schlegel, D., Boroski, B., Adelman-McCarthy, J., Yanny, B., Kent, S., Stoughton, C., et al. 2004, *Astronomische Nachrichten*, 325, 583
- Kowalski, P. M. 2006a, *ApJ*, 641, 488
- 2006b, *ApJ*, 651, 1120
- 2007, *A&A*, 474, 491
- Kowalski, P. M. & Saumon, D. 2004, *ApJ*, 607, 970
- 2006, *ApJ*, 651, L137
- Leggett, S. K., Currie, M. J., Varricatt, W. P., Hawarden, T. G., Adamson, A. J., Buckle, J., Carroll, T., Davies, J. K., et al. 2006, *MNRAS*, 373, 781
- Lépine, S., Rich, R. M., & Shara, M. M. 2005, *ApJ*, 633, L121
- Lépine, S. & Shara, M. M. 2005, *AJ*, 129, 1483
- Lépine, S., Shara, M. M., & Rich, R. M. 2003, *AJ*, 126, 921
- Levine, S. E. 2005, *AJ*, 130, 319
- Liebert, J., Dahn, C. C., & Monet, D. G. 1988, *ApJ*, 332, 891
- Lupton, R. H., Gunn, J. E., & Szalay, A. S. 1999, *AJ*, 118, 1406
- Luyten, W. J. 1974, in *IAU Symposium*, Vol. 61, *IAU Symp. 61: New Problems in Astrometry*, ed. W. Gliese, C. A. Murray, & R. H. Tucker, 169
- Monet, D. G., Levine, S. E., Canzian, B., Ables, H. D., Bird, A. R., Dahn, C. C., Guetter, H. H., Harris, H. C., et al. 2003, *AJ*, 125, 984
- Munn, J. A., Monet, D. G., Levine, S. E., Canzian, B., Pier, J. R., Harris, H. C., Lupton, R. H., Ivezić, Ž., et al. 2004, *AJ*, 127, 3034
- Oppenheimer, B. R., Hambly, N. C., Digby, A. P., Hodgkin, S. T., & Saumon, D. 2001a, *Science*, 292, 698
- Oppenheimer, B. R., Saumon, D., Hodgkin, S. T., Jameson, R. F., Hambly, N. C., Chabrier, G., Filippenko, A. V., Coil, A. L., et al. 2001b, *ApJ*, 550, 448
- Oswalt, T. D., Smith, J. A., Wood, M. A., & Hintzen, P. 1996, *Nature*, 382, 692
- Pier, J. R., Munn, J. A., Hindsley, R. B., Hennessy, G. S., Kent, S. M., Lupton, R. H., & Ivezić, Ž. 2003, *AJ*, 125, 1559
- Richards, G. T., Fan, X., Newberg, H. J., Strauss, M. A., Vanden Berk, D. E., Schneider, D. P., Yanny, B., Boucher, A., et al. 2002, *AJ*, 123, 2945
- Roche, P. F., Lucas, P. W., Mackay, C. D., Eteddgui-Atad, E., Hastings, P. R., Bridger, A., Rees, N. P., Leggett, S. K., et al. 2003, in *SPIE Conference*, Vol. 4841, *Instrument Design and Performance for Optical/Infrared Ground-based Telescopes*, ed. M. Iye & A. F. M. Moorwood, 901–912
- Saumon, D. & Jacobson, S. B. 1999, *ApJ*, 511, L107
- Sesar, B., Svilković, D., Ivezić, Ž., Lupton, R. H., Munn, J. A., Finkbeiner, D., Steinhardt, W., Siverd, R., et al. 2006, *AJ*, 131, 2801
- Skrutskie, M. F., Cutri, R. M., Stiening, R., Weinberg, M. D., Schneider, S., Carpenter, J. M., Beichman, C., Capps, R., et al. 2006, *AJ*, 131, 1163
- Smith, J. A., Tucker, D. L., Kent, S., Richmond, M. W., Fukugita, M., Ichikawa, T., Ichikawa, S., Jorgensen, A. M., et al. 2002, *AJ*, 123, 2121
- Stoughton, C., Lupton, R. H., Bernardi, M. B., Blanton, M. R., Burles, S., Castander, F. J., Connolly, A. J., Eisenstein, D. J., et al. 2002, *AJ*, 123, 485
- Tucker, D. L., Kent, S., Richmond, M. W., Annis, J., Smith, J. A., Allam, S. S., Rodgers, C. T., Stute, J. L., et al. 2006, *Astronomische Nachrichten*, 327, 821
- York, D. G., Adelman, J., Anderson, J. E., Anderson, S. F., Annis, J., Bahcall, N. A., Bakken, J. A., Barkhouser, R., et al. 2000, *AJ*, 120, 1579

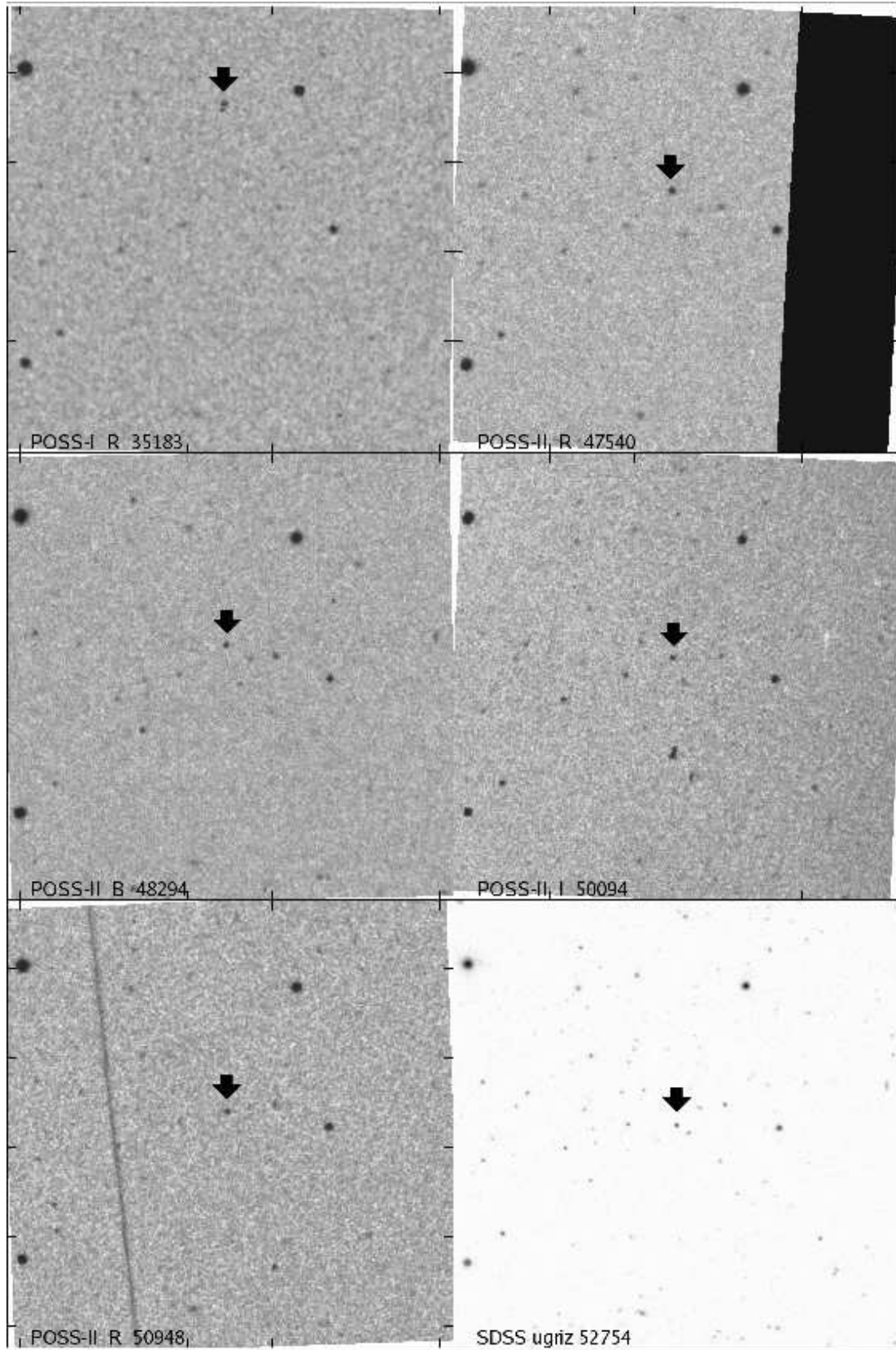


FIG. 1.— Imaging of J1102+4113 (just below each arrow) at six different epochs, centered on its position in the epoch of the SDSS image at lower right. The image source, equivalent passband, and Modified Julian Date (MJD) are indicated in each image. J1102+4113 moves from the top middle to the center of the images over time. Each image is $5' \times 5'$ in size, with North up and East at left.

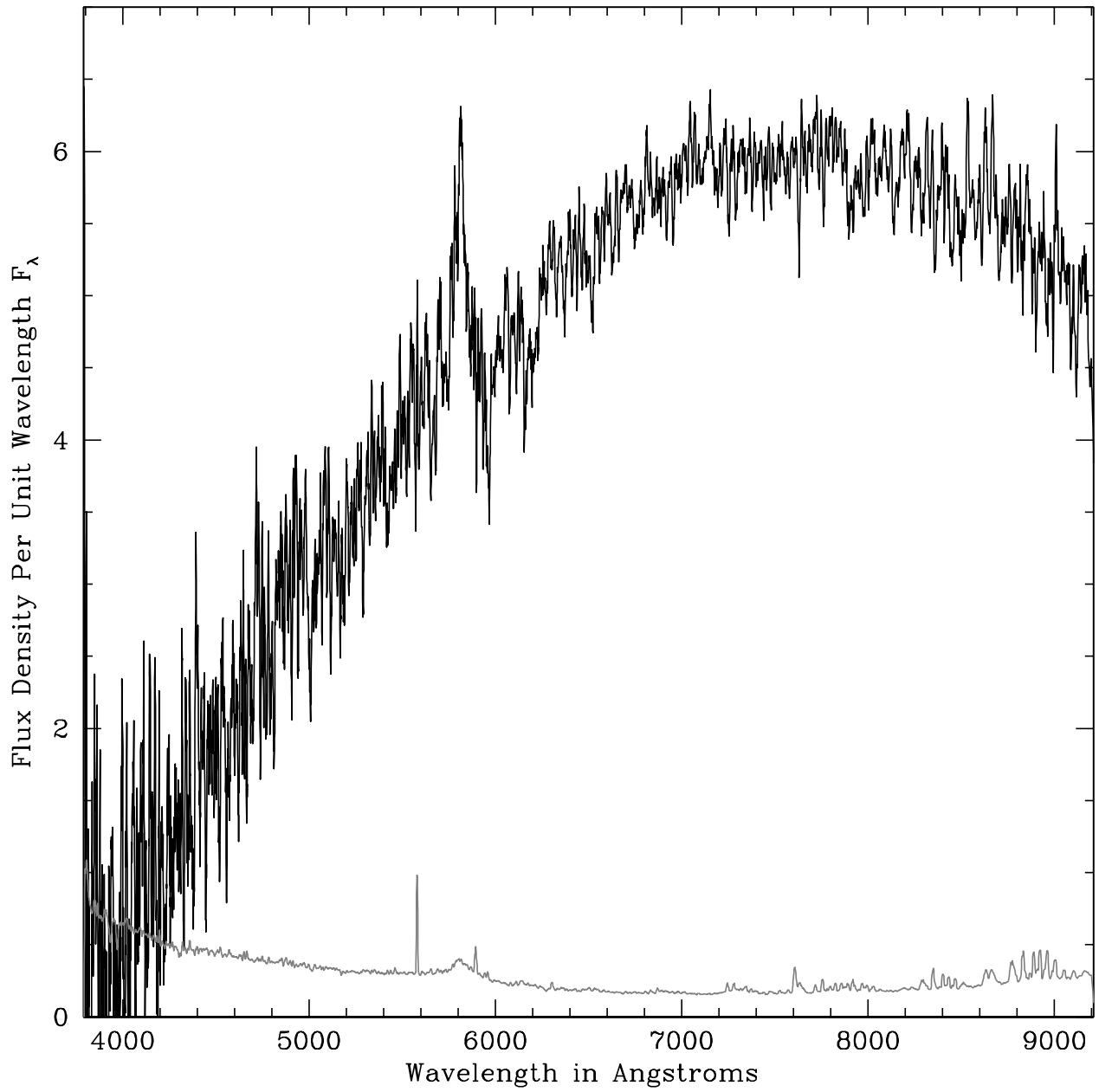


FIG. 2.— Full SDSS spectrum of J1102+4113, smoothed by a 7 pixel boxcar, plotted as F_λ (in units of $10^{-17} \text{ erg s}^{-1} \text{ cm}^{-2} \text{ \AA}^{-1}$) versus wavelength in Å. The uncertainty at each pixel is plotted along the bottom.

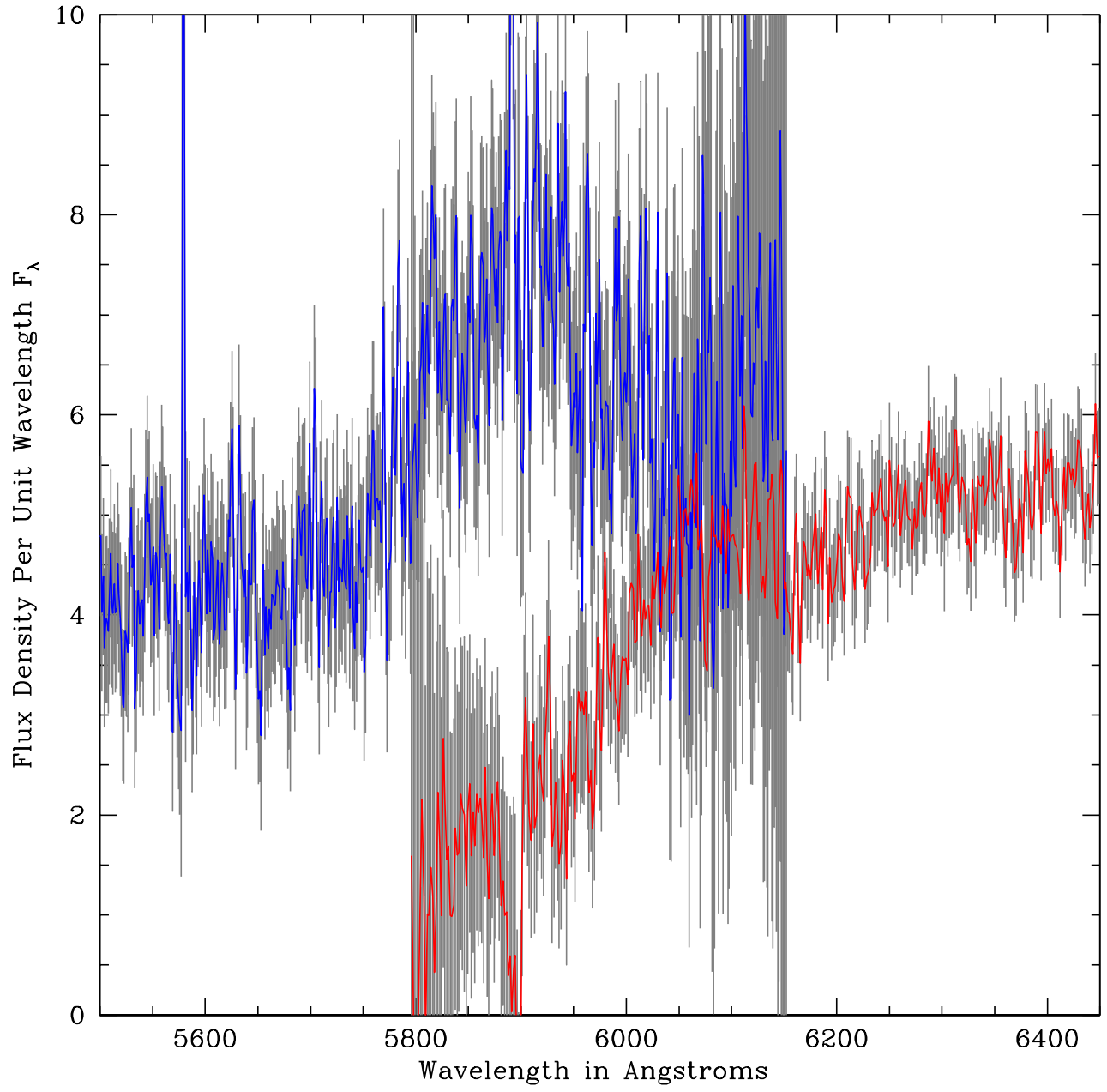


FIG. 3.— Average spectra of J1102+4113 from the blue-wavelength SDSS spectrograph (in blue) and the red-wavelength SDSS spectrograph (in red), along with $\pm 1\sigma$ error bars (in gray). The discrepant flux levels in the two spectra between 5800–6000 Å cast doubt on the reality of the emission feature at 5750–5900 Å in the combined spectrum.

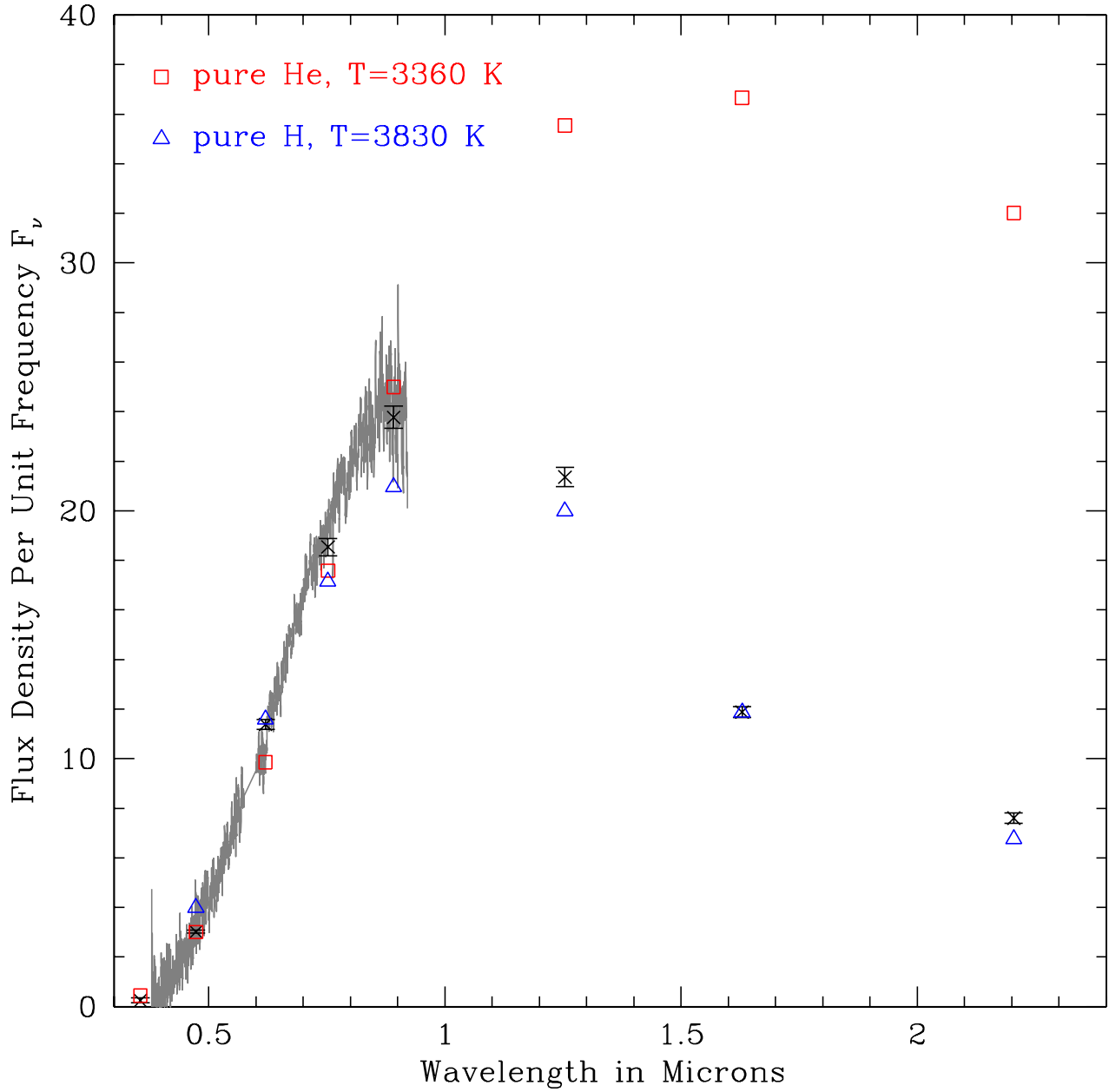


FIG. 4.— Observed spectrum (plotted as F_ν in units of $\text{erg s}^{-1} \text{cm}^{-2} \text{Hz}^{-1}$ versus wavelength in microns), observed photometry and synthetic model photometry of J1102+4113. The SDSS spectrum is shown as the dark gray line and the associated uncertainties as the light gray line. The emission feature we believe to be spurious has been interpolated over. The observed photometry of J1102+4113 is shown as the black error bars. Blue triangles are synthetic photometry from the best-fit pure-H model. Red squares are synthetic photometry from a pure-He model fit to the optical data only.

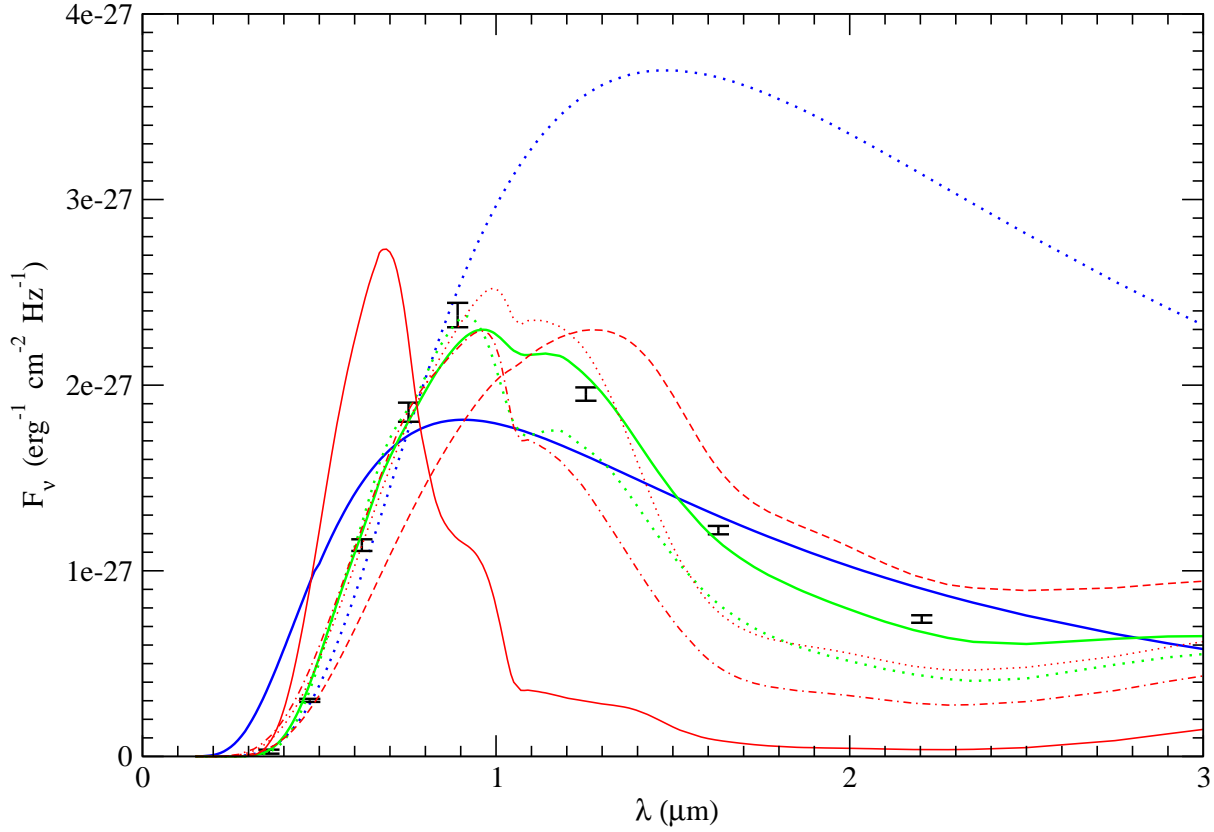


FIG. 5.— Synthetic spectra of pure H, pure He and mixed H/He models, all assuming $\log g = 8$. Fits to all data yield $T_{\text{eff}}=3830$ K for pure H (solid green) and $T_{\text{eff}}=5381$ K for pure He (solid blue). Fits to optical data only yield $T_{\text{eff}}=3450$ K for pure H (dotted green) and $T_{\text{eff}}=3360$ K for pure He (dotted blue). Helium-dominated models with $T_{\text{eff}}=3500$ K are shown by the red lines, with hydrogen contents as follows: $\log \text{H}/\text{He} = -3$ (solid), -4 (dash-dotted), -5 (dotted) and -5.5 (dashed).

TABLE 1
PHOTOMETRY OF SDSS J110217.48+411315.4

Source	MJD	$u \pm \sigma_u$	$g \pm \sigma_g$	$r \pm \sigma_r$	$i \pm \sigma_i$	$z \pm \sigma_z$	$J \pm \sigma_J$	$H \pm \sigma_H$	$K \pm \sigma_K$	$u - g$	$g - z$
POSS1	35183.7938	...	20.59
POSS1	35183.8321	18.58
POSS2	47540.9117	18.67
POSS2	48001.6992	...	20.26
POSS2	48294.8804	...	unavailable
POSS2	50094.9138	18.41
2MASS	50912.8346	17.78 ± 0.76	17.37 ± 0.92	17.52 ± 1.81
POSS2	50948.6813	unavailable
SDSS	52754.1402	23.01 ± 0.48	20.20 ± 0.02	18.76 ± 0.02	18.21 ± 0.02	17.93 ± 0.02	2.81 ± 0.48	2.27 ± 0.03
UKIRT	54456.1192	17.24 ± 0.02	17.33 ± 0.02	17.34 ± 0.03

NOTE. — Optical magnitudes are on the AB system (but see text), and 2MASS and UKIRT magnitudes on the Vega system. 2MASS magnitudes use the 2MASS filter system (Skrutskie et al. 1997) and UKIRT magnitudes use the MKO filter system (Ghinassi et al. 2002). POSS magnitudes have been recalibrated to the indicated SDSS filter (Sesar et al. 2006). SDSS magnitudes are point-spread-function (PSF) magnitudes, but have been converted from asinh magnitudes (Lupton, Gunn, & Szalay 1999) to traditional magnitudes, using the information in Table 21 of Stoughton et al. (2002). For this object, the difference is significant only in the u band.